Geochemical Perspectives Letters

Rise of major subaerial landmasses about 3.0 to 2.7 billion years ago

C.-T. Liu[1], Y.-S. He[1*]

OPEN ACCESS

doi: 10.7185/geochemlet.2115

Abstract

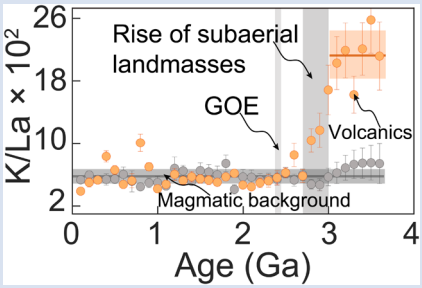

The emergence of subaerial landmasses should have inevitably modulated the chemical composition of the atmosphere-ocean and long term climate. However, it remains controversial when major subaerial landmasses first emerged in Earth's history. Here we show that the mean K/La of globally continental mafic volcanic rocks declined from a fairly high value (~2125) to a magmatic background (~582, indicated by continental mafic plutonic rocks) during 3.0–2.7 Ga. It can only be explained by a progressive reduction in the proportion of submarine hydrothermally altered mafic volcanic samples and thus records a gradual rise of major subaerial landmasses from 3.0 to 2.7 Ga, likely to a present day level since 2.7 Ga. The rise and maintaining of major subaerial landmasses were intrinsically controlled by a dynamic balance of mountain building processes dominantly driven by plate tectonics and subsidence due to weathering erosion and thermal relaxation.

Received 4 December 2020 | Accepted 24 March 2021 | Published 25 May 2021

Introduction

Determining when major subaerial landmasses first emerged and how they rose is the key to understand secular evolution of Earth's ecosystem, but remains challenging. Static models considering multiple parameters (*e.g.*, crustal thickness, density and mantle potential temperature) suggest the rise of major subaerial landmasses from the late Archean to the Neoproterozoic (Flament *et al.*, 2008; Lee *et al.*, 2017). Exposed landmasses have been traced back to as early as ~3.5 Ga (*e.g.*, detrital sediments in the East Pilbara Craton; Buick *et al.*, 1995; Campbell and Davies, 2017), as indicated by geological records of uplift-subsidence cycles (*e.g.*, in the East Pilbara Craton during ~3.5–3.2 Ga; Campbell and Davies, 2017). Early subaerial landmasses may have experienced subsidence and eventually submerged below sea level again, due to crustal erosion and thermal relaxation of continental lithospheric mantle root (Lee *et al.*, 2017). Accordingly, it remains unclear to what extent sporadic geological records can reflect the relative proportion of subaerial landmasses with time.

An increase in subaerial large igneous provinces (LIPs) and a stepwise change of trip-oxygen-isotope ($\Delta^{17}O$) composition of shales indicate major landmasses could have rapidly emerged above sea level at the Archean-Proterozoic boundary (Kump and Barley, 2007; Bindeman *et al.*, 2018). Most intriguingly, it was coincident with Earth's first blast of molecular oxygen (*i.e.* the Great Oxidation Event (GOE)) and has been proposed as a key driving force for the GOE, probably by increasing oxidised subaerial volcanic gases (Kump and Barley, 2007; Gaillard *et al.*, 2011) and decreasing O_2 sinks (*e.g.*, H_2, CH_4) of weathering and alteration (Smit and Mezger, 2017). Both the number of subaerial LIPs and the $\Delta^{17}O$ values of shales, however, appear too muted to reveal the emergence of subaerial landmasses. Here we show the mean K/La of global continental mafic volcanic rocks as a novel proxy to unravel the emergence history of subaerial landmasses.

Rationale & Results

As highly incompatible elements, K and La do not fractionate from each other significantly during mafic magma processes. In contrast, K and La behaviour are very different during weathering and alteration at the surface. K is water-soluble and can thereby be easily removed during chemical weathering, while La is largely insoluble and thus immobile in this process. Weathered subaerial mafic rocks thus on average have depleted K/La (Ma *et al.*, 2007). With input from riverine runoff and high temperature (>100 or 150 °C) submarine hydrothermal processes (Hofmann and Harris, 2008; Staudigel, 2014), K is highly enriched relative to La in seawater. For submarine magma eruptions, the K/La of altered mafic volcanic rocks can be strongly elevated during low temperature hydrothermal alteration (<100 or 150 °C) with seawater (*e.g.*, hydrothermally altered basalts; Fig. 1) (Hofmann and Harris, 2008; Staudigel, 2014; Supplementary Information). Therefore, mafic volcanic rocks in submarine eruptions are expected to possess systematically higher K/La compared to subaerial eruptions. Accordingly, the mean K/La of global continental mafic volcanic rocks could be an ideal proxy to track the relative proportion of submarine to subaerial eruptions over time.

[1] State Key Laboratory of Geological Processes and Mineral Resources, China University of Geosciences (Beijing), Beijing 100083, China
* Corresponding author (email: heys@cugb.edu.cn)

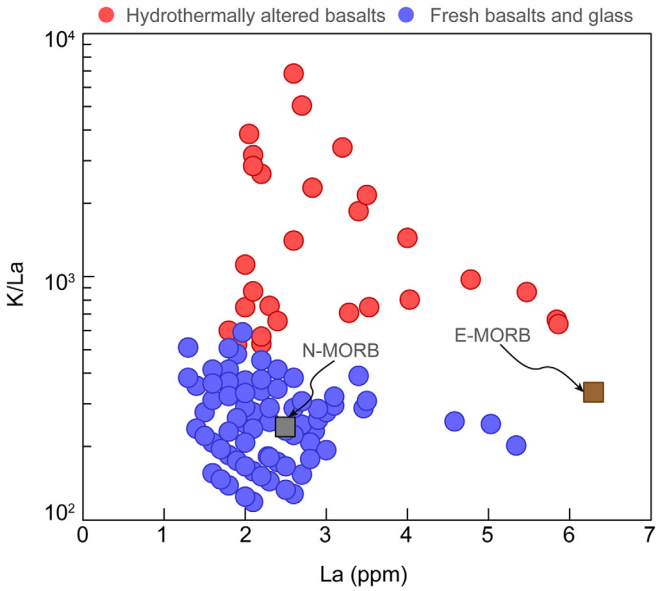

Figure 1 K/La of fresh and hydrothermally altered basalts, exemplified by DSDP and ODP sites 417A, 417D, 418A, 801C, 843B, 1140D and 1149B (see Supplementary Information). Mean normal mid-ocean ridge basalts (N-MORB) and enriched mid-ocean ridge basalts (E-MORB) are from Sun and McDonough (1989).

The weighted bootstrap re-sampling method with Monte Carlo simulations was applied to reveal secular changes in the K/La of less differentiated (SiO_2: 43–51 wt. %) global continental mafic volcanic and plutonic rocks (Fig. S-1) (Keller and Schoene, 2012; Supplementary Information). Mean K/La values of continental igneous rocks were calculated in 100 Ma bins with uncertainty of 1 standard error of the mean (1 s.e.m.) (Fig. 2a, Table S-1). Mafic plutons intruded at depths and thus have been least affected by superficial seawater-rock interactions (Fig. S-2). Accordingly, these rocks can serve as a magmatic background, which yields a nearly constant mean K/La since 3.6 Ga (582 ± 92, 1 standard deviation; 1 s.d.), whereas the mean K/La of mafic volcanic rocks exhibits a substantial change through time. What is striking in mafic volcanic rocks is much higher mean K/La at pre-3.0 Ga—yielding an average value of 2125 ± 309 (1 s.d.)—that progressively decline to near the magmatic background (584 ± 83, 1 s.e.m.) at 2.7 Ga. Three transient positive excursions of K/La have been identified for post-2.7 Ga mafic volcanic rocks, *i.e.* at 0.4, 0.8 and 2.6 Ga, coincident with global tectono-magmatism lulls (Voice *et al.*, 2011; Hawkesworth *et al.*, 2017). Without considering these excursions, the mean K/La of post-2.7 Ga mafic volcanic rocks yield an average of 536 ± 74 (1 s.d.) statistically lower than the magmatic background (*t* test, $p < 0.01$). It indicates distinguishable K depletion relative to La in post-2.7 Ga volcanic rocks relative to their intrusive equilibrants (Fig. 2a).

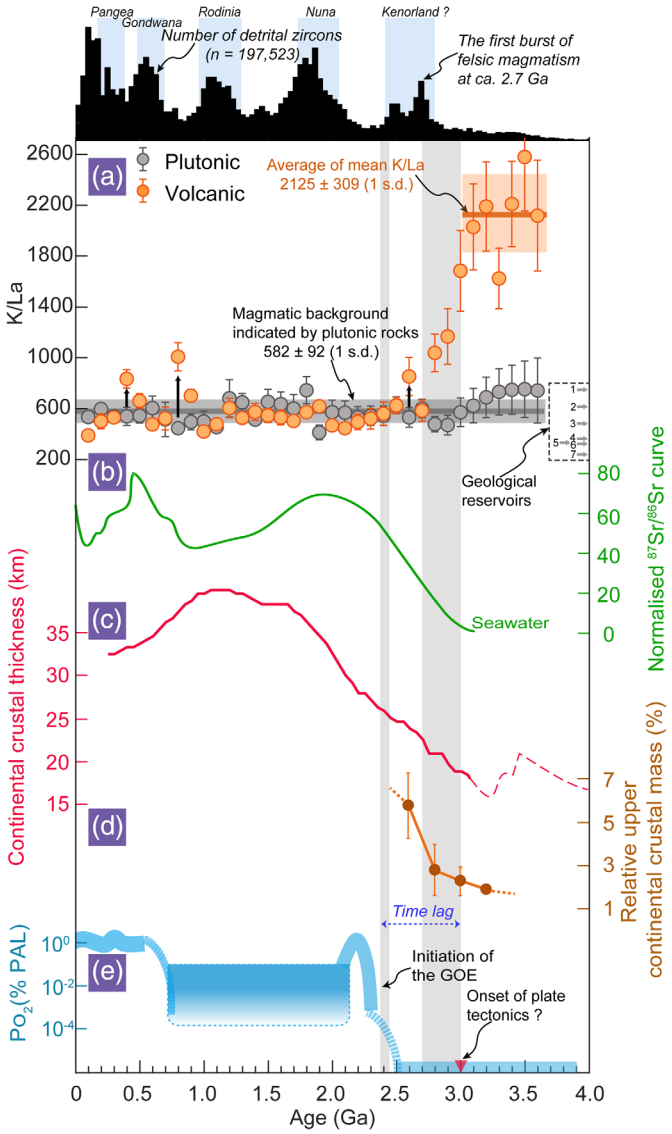

Figure 2 **(a)** Secular mean K/La evolution of global continental mafic volcanic and plutonic rocks. Error bars show 1 s.e.m. uncertainties. Modern geological reservoirs are shown as grey arrows with numbers: (1) upper continental crust, (2) continental arc basalts, (3) lower continental crust, (4) primitive mantle, (5) E-MORB, (6) ocean island basalts (OIB), (7) N-MORB (Sun and McDonough, 1989; Kelemen *et al.*, 2014; Rudnick and Gao, 2014). Secular changes in **(b)** normalised seawater $^{87}Sr/^{86}Sr$ curve (Shields *et al.*, 2007), **(c)** the juvenile continental crustal thickness (Dhuime *et al.*, 2015), **(d)** the upper continental crustal mass (Tang *et al.*, 2016), and **(e)** atmospheric O_2 level (Lyons *et al.*, 2014) are also shown for comparison. Global detrital zircon U-Pb age distribution (Voice *et al.*, 2011) is plotted at the top of the figure, with the periods of supercontinents assembly (Hawkesworth *et al.*, 2017).

Discussion

With the development of plate tectonics (Tang *et al.*, 2016), differentiation in subduction zones and recycling of crustal materials created substantial mantle heterogeneity. On the one hand, influx of more K relative to La into the mantle wedge *via* aqueous fluids derived from subducted sediments and oceanic slabs (Kelemen *et al.*, 2014), tends to produce arc basalts with elevated K/La (*e.g.*, average of continental arc basalts; Fig. 2a). On the other hand, recycling of dehydrated crustal materials can account for some intra-plate basalts with depleted K/La (*e.g.*, average K/La values of Deccan Traps and Siberia LIPs are ~201 and ~161, respectively; Farmer, 2014). However, development of mantle reservoirs with differentiated K/La (*e.g.*, OIB, N-MORB, E-MORB; Sun and McDonough, 1989) appears not to have significantly changed the mean K/La of global mafic magmas with time, as illustrated by nearly constant mean K/La of mafic plutons since 3.6 Ga (Fig. 2a).

Crustal contamination can elevate K/La of continental mafic magmas to various extents by interaction with felsic continental crust with a higher K/La (Fig. 2a). On the contrary, K_2O/Na_2O of felsic continents increases since ~3.0 Ga reaching a modern

value at ~2.5 Ga (Fig. S-3). Contamination by felsic continental crust thus cannot explain the nearly contemporaneous decline in the mean K/La of mafic volcanic rocks. Further, mean K/La values of global mafic volcanic rocks at pre-2.7 Ga are too high (~1039–2580; Table S-1) to be explained by crustal contamination, as the mean K/La of the modern upper continental crust is only ~750 (Rudnick and Gao, 2014; Fig. 2a). Archean mafic volcanic and plutonic samples could both have been subjected to metamorphism. However, the nearly invariable mean K/La of mafic plutonic rocks over time indicates that metamorphism may have not significantly changed mean K/La of global mafic rocks.

The mean K/La of mafic volcanic rocks prior to ~3.0 Ga is too high to be subjected to any magmatic and metamorphic origin. Instead, such high values, to our knowledge, can only be explained by influence of widespread low temperature seawater-rock interactions on these mafic volcanic rocks (Figs. 1, S-2). Therefore, the remarkably elevated mean K/La of pre-3.0 Ga mafic volcanic rocks reveals magma eruptions predominantly at a submarine environment (Fig. 3a), supporting the consensus that most early Archean landmasses were still below sea level (Bindeman *et al.*, 2018). The mantle-like seawater $^{87}Sr/^{86}Sr$ compositions in pre-3.0 Ga (Shields, 2007; Fig. 2b) may also reflect limited erosion of proto-landmasses and a largely submarine state for early Archean landmasses.

Potassium mobility could be quite different during anoxic *versus* oxic alteration of basalts (Jagoutz, 2012). Saponite forms in anoxic altered basalts while celadonite forms in oxic altered basalts. The former mineral contains a much lower K_2O content than the latter one. Therefore, transition from widespread anoxic to oxic alteration across the GOE would predict a systematic increase in the K/La of global mafic volcanic rocks, which is inconsistent with the reverse trend observed in Figure 2a. Instead, the progressive decrease in mean K/La of mafic volcanic rocks during ~3.0–2.7 Ga may reflect a gradual decline in the proportion of magmas that erupted at submarine environments and experienced hydrothermal alteration, in other words, the emergence of subaerial landmasses (Fig. 3b). After this transition, the relatively steady mean K/La of mafic volcanic rocks suggests that, on the whole, the area of subaerial landmasses has not significantly changed since ~2.7 Ga. Statistical analysis on the mean K/La of global mafic volcanic and plutonic rocks thus provides a compelling record for the rise of major subaerial landmasses during ~3.0–2.7 Ga, likely to a present day level since ~2.7 Ga (Figs. 2a, 3b).

The gradual rise of major subaerial landmasses during ~3.0–2.7 Ga can be supported by multiple geological observations. Emergence of large subaerial landmasses initially occurred at ~3.0 Ga at the Kaapvaal craton (*e.g.*, Pongola-Wiwatersrand

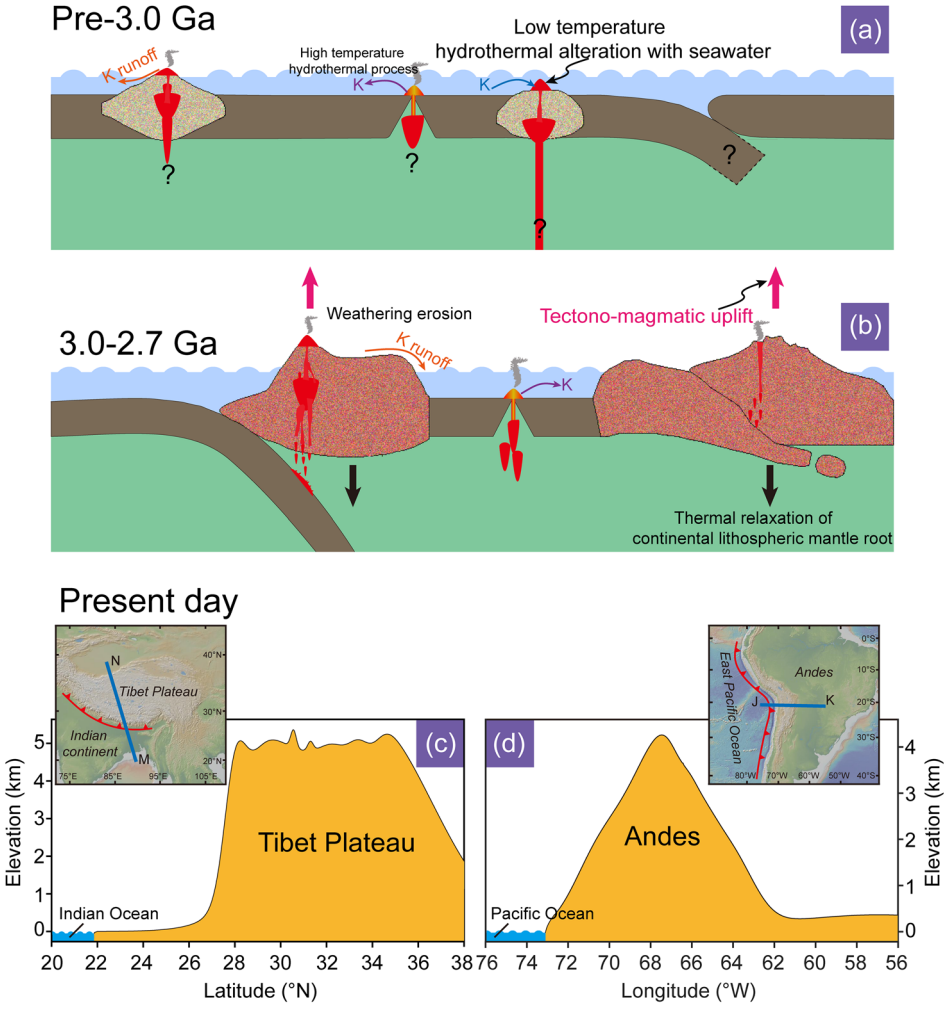

Figure 3 Schematic diagrams illustrating submarine *versus* subaerial states of landmasses in the Archean era. **(a)** Largely submarine state of proto-landmasses at pre-3.0 Ga. **(b)** Rise of subaerial landmasses during ~3.0–2.7 Ga, likely driven by initiation of plate tectonics and assembly of the first supercontinent. These tectono-magmatic events can create high elevations as happens at present day **(c)** Tibet and **(d)** Andes plateaus (see Supplementary Information).

Basin; with an area of hundreds of square kilometres of exposed surface; Kump and Barley, 2007; Korenaga *et al.*, 2017) that then extended to various cratons at ~2.7 Ga (*e.g.*, Kalgoorlie-Kambalda, Abitibi, Slave, Dharwar, Zimbabwe, Wyoming, Kaapvaal and Pilbara; Kump and Barley, 2007; Campbell and Davies, 2017). Increasing seawater $^{87}Sr/^{86}Sr$ isotopic ratios since ~3.0 Ga may reflect more extensive chemical weathering of exposed landmasses at that time (Fig. 2b). The earliest mature detrital zircon age distributions at ~3.0–2.8 Ga also indicates widespread rise of subaerial continents at that time (Reimink *et al.*, 2021).

The area of global subaerial landmasses in Earth's history is regulated by water volume in the hydrosphere, topography differentiation driven by tectono-magmatic events (likely what happens at present day Tibet and Andes plateaus; Fig. 3c,d) as well as processes that eliminate topography difference, *e.g.*, weathering erosion and subsidence due to thermal relaxation of continental lithospheric mantle root (Lee *et al.*, 2017). More than 50 % water in the hydrosphere has been suggested to be returned back to the mantle through subduction in the past (Korenaga *et al.*, 2017). Here we consider that the decline in the total water volume of the hydrosphere was minor during the rise of major subaerial landmasses, as Archean subduction zones, if they existed, were hot and deep subduction of water should have been prevented by prevailing slab melting (Rapp *et al.*, 2003).

Crustal thickness plays an important role in controlling continental elevations (Lee *et al.*, 2017). Rapid growth of crustal thickness as well as felsic components since ~3.0 Ga (Tang *et al.*, 2016; Dhuime *et al.*, 2015) should have increased continental elevations. However, static models with consideration of the crustal thickness, density and mantle potential temperature predict the rise of major subaerial landmasses until the Neoproterozoic (Lee *et al.*, 2017). Instead, the rise of major subaerial landmasses during ~3.0–2.7 Ga can be explained by initiation of plate tectonics (~3.0 Ga; Tang *et al.*, 2016) and assembly of the Earth's first supercontinent (Kenorland), which was marked by the first burst of felsic magmatism at ~2.7–2.5 Ga (Voice *et al.*, 2011; Hawkesworth *et al.*, 2017; Fig. 2). Continuous subduction with the episodic assembly of supercontinents could have provided persistent mountain building processes globally, which must have largely overcome weathering erosion and thermal subsidence to keep the area of global subaerial landmasses nearly constant since ~2.7 Ga. The three K/La positive excursions of mafic volcanic rocks may have recorded several periods with a shrunken area of global subaerial landmasses, which can be explained by weaker orogeny during tectono-magmatic lulls (Fig. 2a).

Submarine landmasses universal in the early Archean, indicated by the extremely high mean K/La of mafic volcanic rocks (Figs. 2a, 3a), with widespread submarine hydrothermal processes and serpentinisation of ultramafic-mafic rocks could have buffered a reduced atmosphere (Smit *et al.*, 2017) and provided proper environments (*e.g.*, N_2, H^+, temperature) for early life (Sleep *et al.*, 2011). For instance, H_2-rich fluids were likely to support the prosperity of methanogens and promote complex organic compounds (biotic or prebiotic life) in pristine seas (Hofmann and Harris, 2008). Intriguingly, the emergence of subaerial landmasses has been proposed as a key driving force for the GOE (Kump and Barley, 2007; Gaillard *et al.*, 2011). A "time lag" is identified here between the rise of major subaerial landmasses and the initiation of the GOE (Lyons *et al.*, 2014; Fig. 2e). This time lag may not be explained by the delayed response of the surficial systems to evolution of the solid Earth, if a steady atmospheric oxygen level could be established at a time scale <50 Ma (Laakso and Schrag, 2014). Accordingly, the emergence of subaerial landmasses during ~3.0–2.7 Ga most likely acted as a precondition rather than a trigger for the GOE. This study suggests alternative mechanisms, *e.g.*, the evolution of oxygen photosynthesis, sedimentary burial of organic carbon (Lyons *et al.*, 2014) and/or deep oxygen cycles driven by volatiles (He *et al.*, 2019), have eventually triggered the GOE.

Author Contributions

Y-SH designed the project. C-TL compiled the datasets and conducted the MATLAB coding. Both authors interpreted the results and prepared the manuscript.

Acknowledgements

The authors appreciate C.B. Keller for his generous and helpful suggestions about theory of the weighted bootstrap resampling method. K. Qu and Y.-Z. Ge provided help with coding. This work was supported by the National Science Foundation of China (Nos. 41688103 and 41730214), the Fundamental Research Funds for the Central Universities (3-7-5-2019-07), the 111 Project of the Ministry of Science and Technology, China (Grant No. BP0719021) and State Key Lab of Geological Processes and Mineral Resources. This is CUGB petrogeochemical contribution No. PGC-201565.

Editor: Cin-Ty Lee

Additional Information

Supplementary Information accompanies this letter at https://www.geochemicalperspectivesletters.org/article2115.

Cite this letter as: Liu, C.-T., He, Y.-S. (2021) Rise of major subaerial landmasses about 3.0 to 2.7 billion years ago. *Geochem. Persp. Let.* 18, 1–5.

References

Bindeman, I.N., Zakharov, D.O., Palandri, J., Greber, N.D., Dauphas, N., Retallack, G.J., Hofmann, A., Lackey, J.S., Bekker, A. (2018) Rapid emergence of subaerial landmasses and onset of a modern hydrologic cycle 2.5 billion years ago. *Nature* 557, 545–548.

Buick, R., Thornett, J.R., McNaughton, N.J., Smith, J.B., Barley, M.E., Savage, M. (1995) Record of emergent continental crust ~3.5 billion years ago in the Pilbara craton of Australia. *Nature* 375, 574–577.

Campbell, I.H., Davies, D.R. (2017) Raising the continental crust. *Earth and Planetary Science Letters* 460, 112–122.

Dhuime, B., Wuestefeld, A., Hawkesworth, C.J. (2015) Emergence of modern continental crust about 3 billion years ago. *Nature Geoscience* 8, 552–555.

Farmer, G.L. (2014) 4.3 – Continental Basaltic Rocks. In: Holland, H.D., Turekian, K.K. (Eds.) *Treatise on Geochemistry*. Second Edition, Elsevier, Oxford, 75–110.

Flament, N., Coltice, N., Rey, P.F. (2008) A case for late-Archaean continental emergence from thermal evolution models and hypsometry. *Earth and Planetary Science Letters* 275, 326–336.

Gaillard, F., Scaillet, B., Arndt, N.T. (2011) Atmospheric oxygenation caused by a change in volcanic degassing pressure. *Nature* 478, 229–232.

Hawkesworth, C.J., Cawood, P.A., Dhuime, B., Kemp, T.I.S. (2017) Earth's continental lithosphere through time. *Annual Review of Earth and Planetary Sciences* 45, 169–198.

He, Y.-S., Meng, X.-N., Ke, S., Wu, H.-J., Zhu, C.-W., Teng, F.-Z., Hoefs, J., Huang, J., Yang, W., Xu, L.-J., Hou, Z.-Q., Ren, Z.-Y., Li, S.-G. (2019) A nephelinitic component with unusual δ^{56}Fe in Cenozoic basalts from eastern China and its implications for deep oxygen cycle. *Earth and Planetary Science Letters* 512, 175–183.

Hofmann, A., Harris, C. (2008) Silica alteration zones in the Barberton greenstone belt: A window into subseafloor processes 3.5–3.3 Ga ago. *Chemical Geology* 257, 221–239.

Jagoutz, O. (2012) Were ancient granitoid compositions influenced by contemporaneous atmospheric and hydrosphere oxidation states? *Terra Nova* 25, 95–101.

Kelemen, P.B., Hanghøj, K., Greene, A.R. (2014) 4.21 – One View of the Geochemistry of Subduction-Related Magmatic Arcs, with an Emphasis on Primitive Andesite and Lower Crust. In: Holland, H.D., Turekian, K.K. (Eds.) *Treatise on Geochemistry*. Second Edition, Elsevier, Oxford, 749–806.

Keller, C.B., Schoene, B. (2012) Statistical geochemistry reveals disruption in secular lithospheric evolution about 2.5 Ga ago. *Nature* 485, 490–493.

Korenaga, J., Planavsky, N.J., Evans, D.A.D. (2017) Global water cycle and the coevolution of the Earth's interior and surface environment. *Philosophical Transactions of the Royal Society A-Mathematical Physical and Engineering Sciences* 375, 20150393.

Kump, L.R., Barley, M.E. (2007) Increased subaerial volcanism and the rise of atmospheric oxygen 2.5 billion years ago. *Nature* 448, 1033–1036.

Laakso, T.A., Schrag, D.P. (2014) Regulation of atmospheric oxygen during the Proterozoic. *Earth and Planetary Science Letters* 388, 81–91.

Lee, C.-T.A., Caves, J., Jiang, H.-H., Cao, W.-R., Lenardic, A., McKenzie, N.R., Shorttle, O., Yin, Q.-Z., Dyer, B. (2017) Deep mantle roots and continental emergence: implications for whole-earth elemental cycling, long-term climate, and the Cambrian explosion. *International Geology Review* 4, 431–448.

Lyons, T.W., Reinhard, C.T., Planavsky, N.J. (2014) The rise of oxygen in Earth's early ocean and atmosphere. *Nature* 506, 307–315.

Ma, J.-L., Wei, G.-J., Xu, Y.-G., Long, W.-G., Sun, W.-D. (2007) Mobilization and re-distribution of major and trace elements during extreme weathering of basalt in Hainan Island, South China. *Geochimica et Cosmochimica Acta* 71, 3223–3237.

Rapp, R.P., Shimizu, N., Norman, M.D. (2003) Growth of early continental crust by partial melting of eclogite. *Nature* 425, 605–609.

Reimink, J.R., Davies, J.H.F.L., Ielpi, A. (2021) Global zircon analysis records a gradual rise of continental crust throughout the Neoarchean. *Earth and Planetary Science Letters* 554, 116654.

Rudnick, R.L., Gao, S. (2014) 4.1 – Composition of the Continental Crust. In: Holland, H.D., Turekian, K.K. (Eds.) *Treatise on Geochemistry*. Second Edition, Elsevier, Oxford, 1–51.

Shields, G.A. (2007) A normalised seawater strontium isotope curve: possible implications for Neoproterozoic-Cambrian weathering rates and the further oxygenation of the Earth. *eEarth* 2, 35–42.

Sleep, N.H., Bird, D.K., Pope, E.C. (2011) Serpentinite and the dawn of life. *Philosophical Transactions of the Royal Society B-Biological Sciences* 366, 2857–2869.

Smit, M.A., Mezger, K. (2017) Earth's early O_2 cycle suppressed by primitive continents. *Nature Geoscience* 10, 788–792.

Staudigel, H. (2014) 4.16 – Chemical Fluxes from Hydrothermal Alteration of the Oceanic Crust. In: Holland, H.D., Turekian, K.K. (Eds.) *Treatise on Geochemistry*. Second Edition, Elsevier, Oxford, 583–606.

Sun, S.-S., McDonough, W.F. (1989) Chemical and Isotopic Systematics of Oceanic Basalts: Implications for Mantle Composition and Processes. *Geological Society, London, Special Publications* 42, 313–345.

Tang, M., Chen, K., Rudnick, R.L. (2016) Archean upper crust transition from mafic to felsic marks the onset of plate tectonics. *Science* 351, 372–375.

Voice, P.J., Kowalewski, M., Eriksson, K.A. (2011) Quantifying the timing and rate of crustal evolution: global compilation of radiometrically dated detrital zircon grains. *Journal of Geology* 119, 109–126.

Geochemical Perspectives Letters

Rise of major subaerial landmasses about 3.0 to 2.7 billion years ago

C.-T. Liu, Y.-S. He

Supplementary Information

The Supplementary Information includes:

- Materials and Methods
- Tables S-1 to S-5
- Figures S-1 to S-3
- Supplementary Information References

Materials and Methods

Data compilation and filtering

Mesozoic basalts with or without low-temperature hydrothermal alteration (Fig. 1) were from Deep Sea Drilling Program (DSDP) and Ocean Drilling Program (ODP) (Emmermann and Puchelt, 1980; Joron *et al.*, 1980; King *et al.*, 1993; Fisk *et al.*, 2002; Kelley *et al.*, 2003) with glass compiled from Bergmanis *et al.* (2007). Data is compiled in Table S-2. Modern seafloor hydrothermal alteration studies reveal that low-temperature hydrothermally altered oceanic basalts can strongly enrich in some elements (*e.g.*, K, Rb, Li, Cs) probably due to the formation of secondary clay minerals (*e.g.*, smectite) during alteration (Emmermann and Puchelt, 1980; Jeffrey and Jose, 1984). However, elements Rb, especially for Li and Cs are relatively scarce in the complied igneous databases. Further tests can be made when the global igneous databases grow and more samples with combined Rb-Li-Cs contents are reported.

Global continental igneous (comprising mafic volcanic and plutonic rocks) database here (for Fig. 2a) were compiled from Keller and Schoene (2012) and the EarthChem repository (http://www.earthchem.org/, accessed 19 February 2020). To overcome the bias of unintendedly erroneous data, we have checked original publications of all the pre-Archean data and corrected some statistical mistakes, *e.g.*, values of K_2O erroneously replaced as Na_2O in igneous database (Keller and Schoene, 2012) according to Polat and Hofmann (2003). All these volcanic and plutonic data for calculation are compiled in Tables S-3 and S-4, respectively.

Note that those data (~2.1 Ga) from Stepanova *et al.* (2014) were not considered in our compiled mafic plutonic dataset (Table S-5). These MORB-type tholeiitic dikes (dolerite, intrusive rock) formed in an extensional setting (the Karelian Craton, in Finland) associated with opening of the Lapland-Kola and Svecofennian oceans, where they may undergo low-temperature hydrothermal alteration resulting in elevated mean K/La (1867 ± 503, 1 s.e.m.; Table S-5). Given the

scarcity of magmatic records during 2.1-2.2 Ga, incorporation of these data into our calculation yields higher K/La that may reflect hydrothermal alteration of hypabyssal rocks at the regional scale (*e.g.*, the Karelian Craton).

In order to include mantle-derived magmas to the utmost, following Keller and Schoene (2012), firstly we filtered the data set with SiO_2 contents from 43 to 51 wt. % (including komatiites). Fractional crystallization or accumulates of some minerals, *e.g.*, plagioclase, alkali feldspar, apatite etc., may influence K/La of mafic rocks, the data set was further filtered by P_2O_5 (≥0.1 wt. %), Al_2O_3 (≤20 wt. %), and MgO (≥6 wt. %) to minimise the effect of fractional crystallization of apatite and feldspar as well as feldspar cumulation. Igneous rocks older than 3.6 Ga were not taken into consideration because such rock records are too rare to be representative.

Statistical methods

We employed the weighted bootstrap resampling method to minimise spatiotemporal preservation bias and to obtain systematic trends of geochemical averages of global igneous rocks (Keller and Schoene, 2012). Every geochemical variable in the database was implemented by following steps: (1) Each sample in a dataset is attached a weight that is inverse to sample's spatiotemporal density. (2) Every data point for a variable is assumed to follow a Gaussian distribution with a mean equal to the value and the standard deviation estimated from its 1σ (usually assumed 2 % as 1σ error). Each geochemical data was used to be randomly (with Monte Carlo simulations) selected proportional to its sample weight to get resampling dataset. (3) According to each sample's age with its uncertainty, the resampling dataset was divided into 100-million-year bins and then a mean value was calculated for every bin. (4) step (1) to (3) were run 10,000 times. (5) A total mean and one standard error of the mean (1 s.e.m.) were calculated for each bin based on results of 10,000 times simulations. Given the worldwide sample distribution (Fig. S-1), this statistical method provides a robust way to optimise, particularly in the pre-Archean era, heterogeneously spatiotemporal sample distribution (15). Note that when it comes to mean value of a ratio (*e.g.*, K/La), elements K and La were resampled by Monte Carol method respectively, and then converted to a ratio for mean and error calculation.

Compilation of elevation data and data processing

We compiled open-source SRTM 90-m Digital Elevation Data (Fig. 3c,d) from http://srtm.csi.cgiar.org/ and conducted Gaussian Fitting via MATLAB's Curve Fitting Tool to smooth the data. Inserted Background maps of Figure 3c,d were downloaded from GeoMapAPP (http://www.geomapapp.org/).

Data availability

Data analysed for this work is available within the paper and its supplementary materials.

Code availability

MATLAB codes for Figure 2a are available at https://github.com/chuntaoL/secular-K-La-variations.

Supplementary Tables

Table S-1 Mean K/La values of continental mafic volcanic and plutonic rocks were calculated by the weighted bootstrap resampling method (10,000 times) for 100-Ma bins with error bars showing 1 s.e.m. uncertainties.

	Volcanic rocks		Plutonic rocks	
Age (Ma)	Mean K/La	Error (1 s.e.m.)	Mean K/La	Error (1 s.e.m.)
100	390	19	533	37
200	500	58	596	47
300	531	41	538	48
400	835	72	538	73
500	661	56	544	59
600	476	39	604	94
700	523	90	514	135
800	1008	111	444	36
900	702	50	494	62
1000	420	37	498	80
1100	477	29	453	31
1200	605	77	681	144
1300	527	48	649	69
1400	574	68	513	40
1500	546	55	653	100
1600	531	58	635	96
1700	504	47	599	111
1800	572	36	744	108
1900	618	30	411	59
2000	468	36	571	95
2100	446	40	567	92
2200	495	61	531	83
2300	521	81	542	77
2400	561	91	542	77
2500	625	63	625	68
2600	853	149	530	77
2700	584	83	599	74
2800	1039	149	475	61
2900	1168	219	469	77
3000	1684	317	570	114
3100	2028	339	622	136
3200	2190	352	688	160
3300	1624	237	732	183
3400	2209	336	748	194
3500	2580	426	753	223
3600	2117	436	742	258

Table S-2 Geochemical data of basalts with or without low-temperature hydrothermal alteration with seawater.

The data table is available for download (Excel file) at https://www.geochemicalperspectivesletters.org/article2115.

Table S-3 Geochemical data of continental mafic volcanic samples (with filtering of SiO_2 = 43–51 wt. %, MgO ≥ 6 wt. %, Al_2O_3 ≤ 20 wt. %, and P_2O_5 ≥ 0.1 wt. %).

The data table is available for download (Excel file) at https://www.geochemicalperspectivesletters.org/article2115.

Table S-4 Geochemical data of continental mafic plutonic samples (with filtering of SiO_2 = 43–51 wt. %, MgO ≥ 6 wt. %, Al_2O_3 ≤ 20 wt. %, and P_2O_5 ≥ 0.1 wt. %).

The data table is available for download (Excel file) at https://www.geochemicalperspectivesletters.org/article2115.

Table S-5 Geochemical raw data of tholeiitic dikes at the Karelian Craton and mean K/La calculated by the bootstrap method.

The data table is available for download (Excel file) at https://www.geochemicalperspectivesletters.org/article2115.

Supplementary Figures

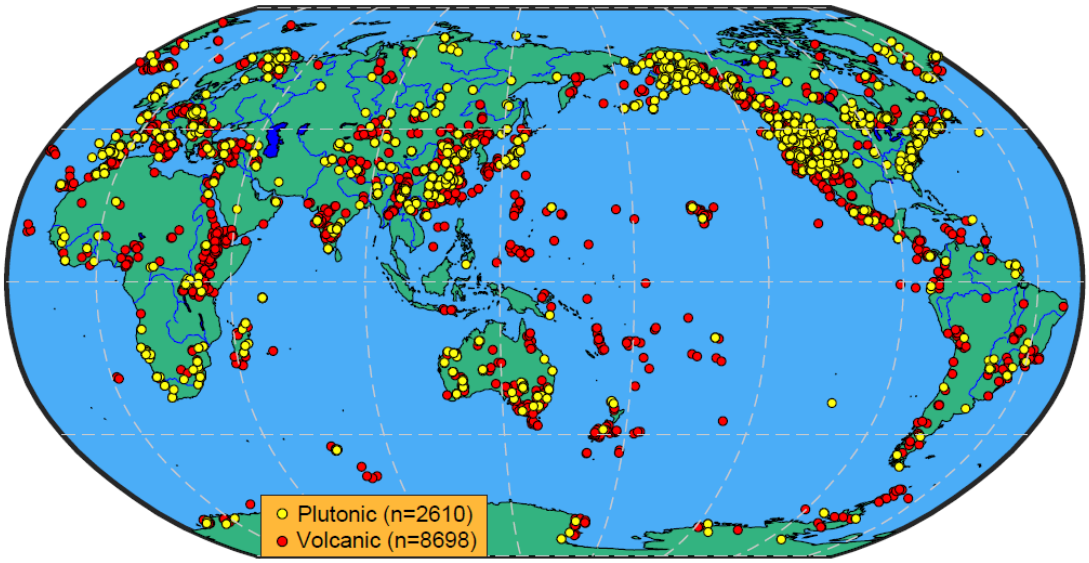

Figure S-1 Global distribution of continental igneous raw samples (listed in Tables S-2 and S-3; with filtering of SiO_2 = 43–51 wt. %, MgO ≥ 6 wt. %, Al_2O_3 ≤ 20 wt. %, and P_2O_5 ≥ 0.1 wt. %).

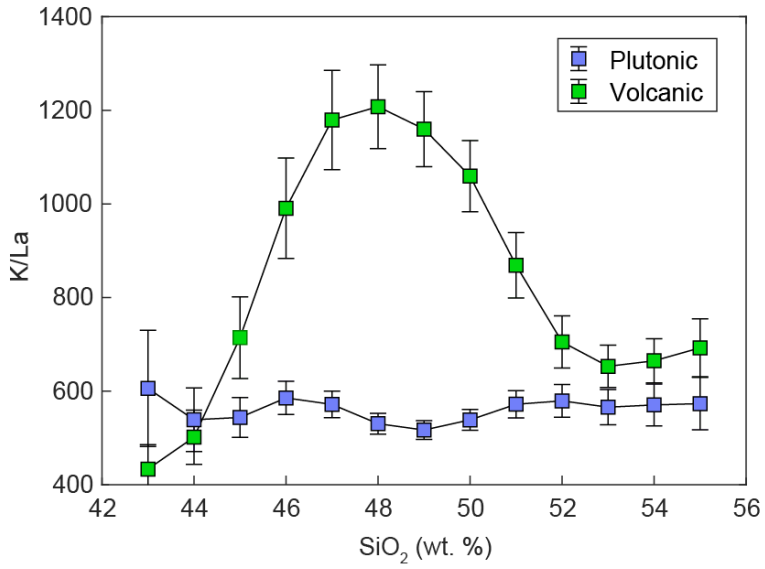

Figure S-2 Diagram of K/La versus SiO_2 for continental mafic volcanic and plutonic rocks. Mean K/La values of mafic volcanic and plutonic rocks were calculated by the weighted bootstrap resampling method (10,000 times) for 1 wt. % SiO_2 intervals with error bars showing 1 s.e.m. uncertainties. Mean K/La of mafic plutonic rocks keeps nearly constant with SiO_2 varying from 43 to 55 wt. %, suggesting that K/La cannot be significantly fractionated during mantle partial melting and differentiation of mafic magmas. While mafic volcanic rocks yield elevated mean K/La values for a given $SiO_2 \geq 45$ wt. %, which most likely reflects that submarine mafic volcanic magmas have more chance to experience low-temperature hydrothermal alteration with seawater. Mafic plutonic rocks were emplaced at depths, thus being least affected by post superficial seawater-rock interaction.

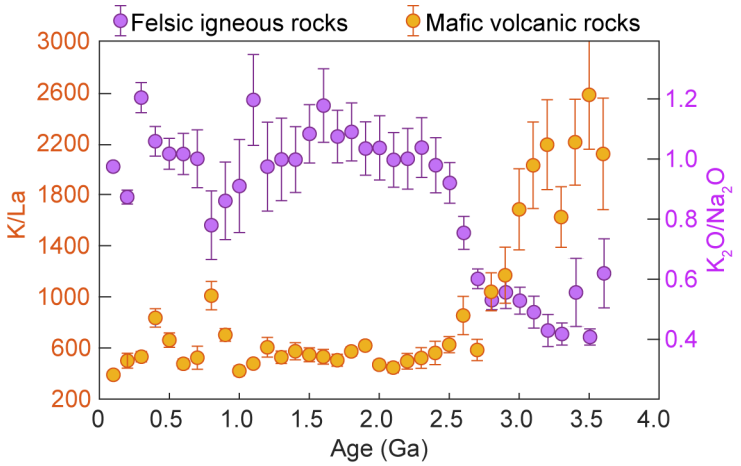

Figure S-3 Secular compositional variations of K/La of mafic volcanic rocks (the same as Fig. 2a in the main text) and K_2O/Na_2O of felsic igneous rocks (modified from Keller and Schoene, 2012). Mean K_2O/Na_2O of felsic igneous rocks increase from ~3.0 to ~2.5 Ga, of which contamination cannot interpret the nearly contemporaneous reduction in mean K/La of mafic volcanic rocks.

Supplementary Information References

Bergmanis, E.C., Sinton, J., Rubin, K.H. (2007) Recent eruptive history and magma reservoir dynamics on the southern East Pacific Rise at 17°30'S. *Geochemistry Geophysics Geosystems* 8, Q12O06.

Emmermann, R., Puchelt, H. (1980) Major and trace element chemistry of basalts from Holes 417D and 418A, Deep Sea Drilling Project Legs 51-53. In: Donelly, T., Francheteau, J., Bryan, W., Robinson, P., Flower, M., Salisbury, M., *et al.* (Eds.) *Initial Reports of the Deep Sea Drilling Project*. U.S. Govt. Printing Office, Washington, 987–1000.

Fisk, M., Kelley, K.A. (2002) Probing the Pacific's oldest MORB glass: mantle chemistry and melting conditions during the birth of the pacific plate. *Earth and Planetary Science Letters* 202, 741–752.

Jeffrey, C.A., Jose, H. (1984) Alteration of the upper oceanic crust, DSDP site 417: mineralogy and chemistry. *Contributions to Mineralogy and Petrology* 87, 149–169.

Joron, J.L., Bollinger, C., Quisefit, J.P., Bougault, H., Treuil, M. (1980) Trace elements in Cretaceous basalts at 25ºN in the Atlantic Ocean: alteration, mantle compositions, and magmatic processes. In: Donelly, T., Francheteau, J., Bryan, W., Robinson, P., Flower, M., Salisbury, M., *et al.* (Eds.) *Initial Reports of the Deep Sea Drilling Project*. U.S. Govt. Printing Office, Washington, 1087–1098.

Kelley, K.A., Plank, T., Ludden, J., Staudigel, H. (2003) Composition of altered oceanic crust at ODP sites 801 and 1149. *Geochemistry Geophysics Geosystems* 4, 8910.

Keller, C.B., Schoene, B. (2012) Statistical geochemistry reveals disruption in secular lithospheric evolution about 2.5 Ga ago. *Nature* 485, 490–493.

King, A.J., Waggoner, D.G., Garcia, M.O. (1993) Geochemistry and petrology of basalts from Leg 136, central Pacific Ocean. In: Wilkens, R.H., Firth, J., Bender, J., *et al.* (Eds.) *Proceedings of the Ocean Drilling Program Scientific Results*. Ocean Drilling Program, College Station, TX, 136, 107–118.

Polat, A., Hofmann, A.W. (2003) Alteration and geochemical patterns in the 3.7-3.8 Ga Isua greenstone belt, West Greenland. *Precambrian Research* 126, 197–218.

Stepanova, A.V., Salnikova, E.B., Puchtel, I.S., Larionova, Yu.O., Larionov, A.N., Stepanov, V.S., Shapovalov, Y.B., Egorova, S.V. (2014) Palaeoproterozoic continental MORB-type tholeiites in the Karelian Craton: Petrology, geochronology, and tectonic setting. *Journal of Petrology* 55, 1719–1751.

Sun, S.-S., McDonough, W.F. (1989) Chemical and Isotopic Systematics of Oceanic Basalts: Implications for Mantle Composition and Processes. *Geological Society London Special Publications* 42, 313–345.